Dynamics of photo-excited electrons in magnetically ordered TbMnO3

Handayani, I. P.; Tobey, R. I.; Janusonis, J.; Mazurenko, D. A.; Mufti, N.; Nugroho, A. A.; Tjia, M. O.; Palstra, T. T. M.; van Loosdrecht, P. H. M.

Published in:
Journal of Physics-Condensed Matter

DOI:
10.1088/0953-8984/25/11/116007

IOP Publishing Journal of Physics: Condensed Matter
J. Phys.: Condens. Matter **25** (2013) 116007 (4pp) doi:10.1088/0953-8984/25/11/116007

Dynamics of photo-excited electrons in magnetically ordered $TbMnO_3$

I P Handayani[1], R I Tobey[1], J Janusonis[1], D A Mazurenko[1], N Mufti[1,3], A A Nugroho[2], M O Tjia[2], T T M Palstra[1] and P H M van Loosdrecht[1]

[1] Zernike Institute for Advanced Materials, University of Groningen, The Netherlands
[2] Faculty of Mathematics and Natural Sciences, Institut Teknologi Bandung, Indonesia

E-mail: p.h.m.van.loosdrecht@rug.nl

Received 18 September 2012, in final form 1 February 2013
Published 19 February 2013
Online at stacks.iop.org/JPhysCM/25/116007

Abstract
Time resolved optical spectroscopy is used to elucidate the dynamics of photodoped spin-aligned carriers in the presence of an underlying magnetic lattice in the multiferroic compound $TbMnO_3$. The transient responses while probing d–d intersite transitions show marked differences along different crystallographic directions, which are discussed in terms of the interplay between the processes of hopping of the photo-injected electrons and the magnetic order in the material.

(Some figures may appear in colour only in the online journal)

The physical properties of 3d transition metal oxides result from an intricate interplay of the lattice, charge, orbital, and spin. In the manganite oxides, for example, this leads to a variety of ordered phases of charges, orbitals, and spins states [1], which in turn drives emergent properties ranging from colossal magneto-resistive phenomena [2] to the occurrence of multiferroicity [3]. Unraveling the underlying interactions that dictate this emergent behavior is not always straightforward using static experiments aimed at ground state properties and excited state spectra. In recent years it has become clear that extending the experimental repertoire to dynamical phenomena leads to valuable new insights, for instance, the potential for temporally decoding the competing interactions [4–6]. One of the most straightforward implementations of this is the investigation of hot electron relaxation following photo-excitation, and its consequences for the transient material properties [4, 7]. As the sample temperature is lowered through a succession of phase transitions, besides the conventional electron–phonon scattering channel, additional scattering channels alter the relaxation dynamics and provide a means for clarifying the array of interactions that dictate behavior. This methodology can be applied in many systems, including those where charge transport is influenced by underlying magnetism, and materials with coupled ferroic properties.

It is the purpose of the present study to investigate the coupling of charge (hopping) transport with magnetic order by probing the dynamics and relaxation processes of the excited material. In addition, we are interested in the relevance of magneto-electric couplings in multiferroic materials to these relaxation dynamics. We have chosen a material which allows us to monitor these relaxation dynamics along orthogonal crystallographic directions with different underlying magnetic orderings. We find, not unexpectedly, that the transport properties along these two directions are considerably different. Using a simple model, we describe the observed dynamics by considering the processes of intersite hopping between nearest neighbors subject to the constraints imposed by the underlying magnetic lattice. In this picture, we see that electron–magnon interactions dominate the relaxation processes in the magnetic state, and find a strong coupling with low-energy magnonic excitations.

The material that we have chosen for our experiment is the canonical multiferroic $TbMnO_3$. The static structural and magnetic properties of the $REMnO_3$ (RE = Gd, Tb, Dy, Ho) multiferroic family, and this material in particular, have been studied at length [8–12]. We focus briefly on the magneto-structural properties as they pertain to our experiment [10, 13, 14]. The small atomic radius of the

[3] Present address: Physics Department, State University of Malang, Indonesia.

Tb^{3+} ion distorts the cubic perovskite structure, giving rise to the most distorted $GdFeO_3$-type lattice of the orthorhombic $REMnO_3$ family. (For a thorough treatise on octahedral tilts, see for example Lufaso and Woodward [15] and Glazer [16].) This structural distortion leads to frustration of the manganese spin degree of freedom due to strong competition between nearest neighbor (NN) and next nearest neighbor (NNN) magnetic interactions [13]. As a consequence, the FM interaction along the *a*-axis decreases and a sinusoidal AFM spin structure is formed along the *b*-direction at the Néel temperature, $T_{N,1} = 41$ K. Below $T_{N,2} = 26$ K, the magnetic structure changes to a *bc*-cycloid with the concurrent appearance of the spontaneous electric polarization along the *c*-axis [8, 11].

The sample for our experiment is a single crystal grown using the floating zone technique [17] which is cut and polished to obtain a *b*-axis surface normal. The crystal size is roughly 3 mm × 2 mm and 0.5 mm thick. With this cut, two distinct magnetic orderings are optically accessible through a 90° rotation of the incoming light polarization: (1) along the ⟨100⟩ crystallographic axis, ferromagnetic NN interactions are present, while (2) along the ⟨001⟩ direction, antiferromagnetic NN interactions are present. Using light tuned to the manganese–manganese d–d transition [18], we probe the magnetic order through the sensitivity of the intersite d–d transition to the underlying magnetic lattice along both directions.

To elucidate the interactions between photo-injected electrons and the magnetic lattice, we performed two-color pump–probe measurements across a wide temperature range encompassing $T_{N,1} = 41$ K and $T_{N,2} = 26$ K. Hot electrons are photo-excited onto the manganese site using 3.0 eV photons, the second harmonic of our laser, which is well tuned to oxygen–manganese charge transfer excitations [18]. Subsequently, the manganese–manganese intersite transition is monitored at 1.5 eV, the fundamental of our laser, which overlaps the nearest neighbor intersite d–d transition. Both beams are derived from our 1 kHz Ti:sapphire amplified laser system (Hurricane, Spectra Physics) which produces 200 fs pulses with a central wavelength of 800 nm. The pump and probe are spatially and temporally overlapped on the sample surface and the pump fluence is 0.1 mJ cm^{-2} for all experiments reported here[4]. In order to probe the response along ferromagnetically and antiferromagnetically coupled directions, the probe light is polarized at 45° with respect to the *a*- and *c*-axes and analyzed by using a Wollaston prism. The temporal dynamics are investigated in the temperature range between 9 and 125 K.

In figure 1 we show transient reflectivities $\frac{\Delta R(t)}{R}$ measured along the *c*-axis (top) and *a*-axis (bottom), as the sample temperature is lowered through the magnetic transition. The observed dynamics along the two axes are markedly different. In particular, the photo-induced state is marked by a reduction in reflectivity along the *a*-axis and an increase in reflectivity along the *c*-axis, while the trend is

[4] The pump fluence is in the linear regime, as checked by fluence dependent experiments.

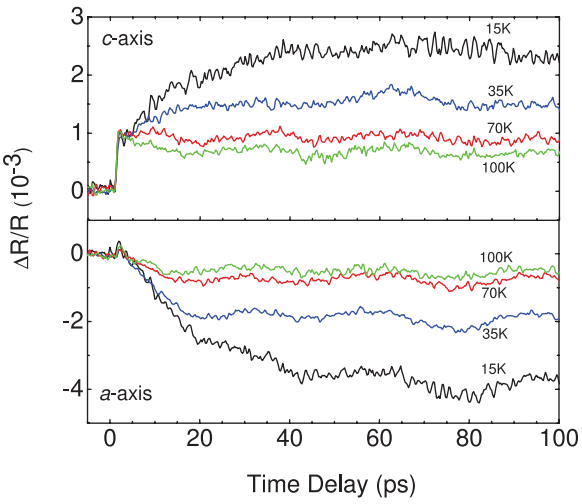

Figure 1. Characteristic transient reflectivity curves along the two principal crystallographic directions for temperatures above and below the magnetic transition at 41 K. We witness along the ferromagnetically coupled *a*-axis a decrease in transient reflectivity, while we witness along the antiferromagnetically coupled *c*-axis an increase in transient reflectivity.

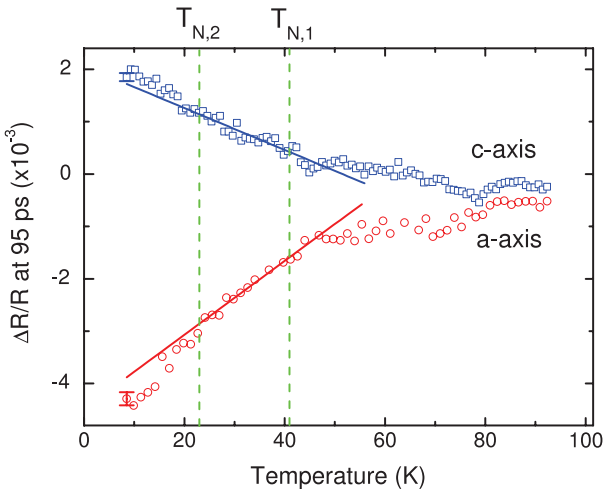

Figure 2. The transient reflectivity probed at 95 ps shows clear changes in amplitude at the first magnetic transition, $T_{N,1}$. Using a solid linear fit between 26 and 42 K, more subtle changes are observed in the amplitude at $T_{N,2}$. Above the magnetic transition the difference in transient reflectivity indicates that short range magnetic interactions persist.

an increase of $\left|\frac{\Delta R_i(t)}{R}\right|_{i=a,c}$ as the temperature is lowered. The two axes are further distinguished by the temperature independent ultrafast response along the *c*-axis, well matched to the pump–probe cross-correlation. We also note a common oscillatory component which is attributed to the generation of acoustic phonons. The responses along both axes persist for longer than 300 ps, the limit of our translation stage.

Further analysis of the transient reflectivity is provided in figure 2, where we show the temperature dependent transient reflectivity in the metastable state, measured at 95 ps time delay. Representative error bars show the standard deviation of the data points in a small time window around the 95 ps time delay. For the *c*-axis data (squares) the sharp jump at zero

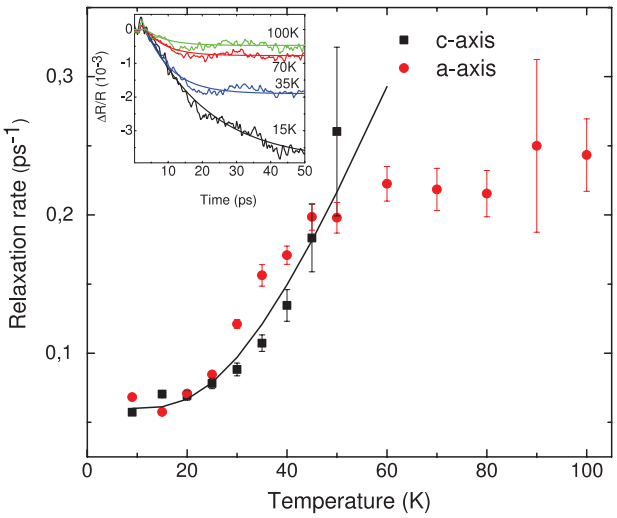

Figure 3. The relaxation rate of photo-injected electrons exhibits an increase in time constant as a function of temperature. Fitting this time constant to a Bose–Einstein distribution for the number of magnons at temperature T, we extract a characteristic energy of 8 meV, well matched to the near zone boundary magnon energy.

time delay is subtracted. The first magnetic phase transition at $T_{N,1} = 41$ K is clearly visible as a change in slope along both axes. Changes at $T_{N,2} = 26$ K are present, but less noticeable. To highlight these more subtle changes, a linear fit in the region between $T_{N,1}$ and $T_{N,2}$ is included. Deviations from linearity are now evident as a slight change in the slope at $T_{N,2}$. Additionally, we observe a difference in signal amplitude above $T_{N,1}$ for the two crystallographic directions, possibly indicative of short range magnetic order that persists for temperatures above the magnetic ordering temperatures. Signatures of such short range order were found by Bastjan *et al* [18] up to 300 K. We note that even above the magnetic ordering temperature, orbital order and structural distortions persist up to 800 K [13, 14], and therefore it is not surprising to see slight deviations along the different axes.

The onset of magnetic ordering is further seen in the extracted time constants, obtained from fitting the time dependence with a single-exponential function, as shown in figure 3. The inset shows such representative curves (copied from figure 1) together with their fit for temperatures spanning the magnetic transitions. Upon entering the magnetic phase at 40 K, the dynamic response slows down dramatically. Above the transition temperature, the onset time scale remains constant up to 100 K, most easily seen in the *a*-axis response. The *c*-axis response is less clear due to the difficulty in fitting caused by the fast component at T_0 (see figure 1). As the temperature is lowered, the time constants along both axes asymptote to a value of $\tau = 17$ ps.

To interpret the observed dynamics we must consider the effects of both the underlying magnetic interactions—the main aim of this paper—and those arising from differences in structure. We first briefly address the jump in reflectivity apparent along the *c*-axis and absent along the *a*-axis, which we can identify as having a non-magnetic origin. The direct indication of this is the absence of temperature dependence in the amplitude of this effect. Furthermore, this fast transient linearly depends on the number of photo-excited electrons, as evidenced by experiments performed at different fluences *(data not shown)*. We therefore attribute this feature to optical intersite d–d transitions induced by the presence of the photo-excited electrons, which is favorable along the *c*-direction due to the out-of-plane nature of the newly occupied orbitals ($x^2 - z^2$ or $y^2 - z^2$). Apart from this instantaneous jump, the 'slow' onset and long lived dynamics are interpreted as arising from the interaction between the photo-excited electron and the underlying magnetic lattice. This is evident in the amplitude of the transient reflectivity at long time delays as shown in figure 2. Changes in the amplitude, manifested as modifications of the slope in figure 2, directly map to the magnetic transitions independently measured in $TbMnO_3$ [11, 17]. We proffer this magnetic interaction as the dominant effect in determining the long lived temporal evolution by noting that the underlying lattice parameters continuously change over the entire temperature range [20], displaying only a modest change at the temperature where we see our largest change in dynamics.

To understand the interaction between the photo-excited electron and the underlying magnetic lattice, we first consider the effects of magnetic ordering on the reflectivity at the probe wavelength. The relevant transitions at 1.5 eV are the intersite d–d transitions $(Mn^{3+}, Mn^{3+}) \rightarrow (Mn^{2+}, Mn^{4+})$. As has been discussed by Bastjan *et al* and Kovaleva *et al* [18, 19], the energy of this transition depends on the spin alignment of the neighboring Mn^{3+} ions. For parallel alignment, as is the case along the *a*-direction, the transition occurs around 1.5–2 eV, whereas for antiparallel alignment (along the *c*-direction) the energy of this transition is increased by Hund's energy. Therefore one expects, for the perfect spin ordered case, the transitions along the *a*-direction to have maximal probability, and those along the *c*-direction to have minimal probability.

Next we consider the effect of photodoping the e_g levels through an oxygen–manganese p–d transition, resulting in the creation of Mn^{2+} ions. Once created, the additional electron which, through Hund's rule coupling, will be spin aligned can in principle hop to different Mn sites leading to a photo-induced hopping conductivity. In the presence of magnetic order, this hopping is expected to be highly anisotropic. Along the *a*- and *b*-directions where the magnetic alignment of neighboring Mn sites is predominantly ferromagnetic, the hopping costs minimal energy, and moreover, will not affect the magnetic order of the system. In contrast to this, hopping along the *c*-direction, where the spin alignment is antiferromagnetic, is prohibited by an energy cost equivalent to Hund's energy unless a spin flip occurs. Therefore, along this direction only magnon-assisted hopping is allowed, which strongly modifies the ground state magnetic order. Each hop of the photo-excited electron along the *c*-direction necessarily modifies the optical response along both axes at 1.5 eV. One hopping process, along *c*, creates a magnonic excitation leading to a decrease in magnetic order. This induced magnetic disorder naturally leads to the observed negative response along the *a*-direction (decrease of NN ferromagnetic alignment) and a positive response along

the *c*-direction (decrease of antiferromagnetic NN alignment). Furthermore, the trend with decreasing temperature towards increasing signal amplitude can be seen in the same light. As the temperature is increased from zero, the thermally induced magnetic disorder in the system increases, reducing the magnitude of the pump induced signal. Finally, the probability of this magnon-assisted hopping process is known to scale with the magnon number density [21] and hence the observed time constant is expected to increase as the temperature is raised.

On the basis of the above discussions, we interpret the transient behavior of the reflectivity presented in figures 2 and 3 as the signature of photo-induced magnon-assisted hopping conductivity leading to a transient reduction of the magnetic order in the material. The rate of decrease of the magnetic order is proportional to the hopping probability and hence to the magnon number density $n(\omega_q, T)$.

Since we are considering hopping to nearest neighbors in the *c*-direction, the relevant magnon frequency, ω_q, dominating the hopping process should be the lowest zone boundary magnon frequency. This is indeed corroborated by the observed temperature dependence of the fitted time constants. The time constants extracted from our fitting procedure are shown in figure 3. The time constant data set is fitted with a Bose–Einstein distribution—combined with a constant to accommodate additional relaxation processes ($[A/\exp(\hbar\omega_q/k_B T) - 1]^{-1} + B$)—between 10 and 41 K, giving the average number density of magnons at temperature T. The characteristic energy extracted from the fit is 8.5 ± 1 meV, well matched to the energy of the zone boundary excitation as observed in [22]. This magnetic excitation is known to disperse from 1.5 meV at the zone center to 8.5 meV at the boundary. In probing the hopping conductivity, there is particular sensitivity to nearest neighbor magnetic alignment, which couples most strongly to the zone boundary excitation.

In conclusion, the physical properties of 3d oxides often depend crucially on the interplay of charge, orbit, spin and lattice. For $TbMnO_3$ this leads to insulating behavior and the formation of complex magnetic ground states, including a multiferroic one. Here we have shown that one can unravel details of these interactions through relatively simple time resolved experiments, which in particular show the intrinsic correlation between hopping conductivity and magnetic correlations. The results presented here are expected to be relevant not only for $TbMnO_3$, but certainly also for conducting chemically doped variants of this material, as well as for many other 3d oxide compounds.

Acknowledgments

IPH gratefully acknowledges financial support by NUFFIC through the Netherlands Fellowship Programmes and the Schlumberger Foundation through the Faculty for the Future Programme. This work was supported by the research programme of the Foundation for Fundamental Research on Matter (FOM), which is part of the Netherlands Organization for Scientific Research (NWO).

References

[1] Tokura Y and Nagaosa N 2000 *Science* **288** 462–8
[2] Ramirez A P 1997 *J. Phys.: Condens. Matter* **9** 8171–99
[3] Cheong S W and Mostovoy M 2007 *Nature Mater.* **6** 13–20
[4] Averitt R D, Lobad A I, Kwon C, Trugman S A, Thorsmølle V K and Taylor A J 2001 *Phys. Rev. Lett.* **87** 017401
[5] Matsubara M, Okimoto Y, Ogasawara T, Tomioka Y, Okamoto H and Tokura T 2007 *Phys. Rev. Lett.* **99** 0207401
[6] Boeglin C, Beaurepaire E, Halté V, López-Flores V, Stamm C, Pontius N, Dürr H A and Bigot J-Y 2010 *Nature* **465** 458
[7] Beaurepaire E, Merle J-C, Daunois A and Bigot J-Y 1999 *Phys. Rev. Lett.* **76** 4250
[8] Quezel S, Tcheou F, Rossat-Mignod J, Quezel G and Roudaut E 1977 *Physica* B+C **86–88** 916–8
[9] Alonso J A, Martinez-Lope M J, Casais M T and Fernandez-Diaz M T 2000 *Inorg. Chem.* **39** 917
[10] Kimura T, Goto T, Shintani H, Ishizaka K, Arima T and Tokura Y 2000 *Nature* **426** 55
[11] Kajimoto R, Yoshizawa H, Shintani H, Kimura T and Tokura Y 2000 *Phys. Rev.* B **70** 012401
[12] Kenzelmann M, Harris A B, Jonas S, Broholm C, Schefer J, Kim S B, Zhang C L, Cheong S-W, Vajk O P and Lynn J W 2005 *Phys. Rev. Lett.* **95** 087206
[13] Kimura T, Ishihara S, Shintani H, Arima T, Takahashi K T, Ishizaka K and Tokura Y 2003 *Phys. Rev.* B **68** 060403
[14] Zhou J S and Goodenough J B 2006 *Phys. Rev. Lett.* **96** 247202
[15] Lufaso M W and Woodward P M 2004 *Acta Crystallogr.* B **60** 10
[16] Glazer A M 1972 *Acta Crystallogr.* B **28** 3384
[17] Mufti N, Nugroho A A, Blake G R and Palstra T T M 2008 *Phys. Rev.* B **78** 024109
[18] Bastjan M, Singer S G, Neuber G, Eller S, Aliouane N, Argyriou D N, Cooper S L and Rübhausen M 2008 *Phys. Rev.* B **77** 193105
[19] Kovaleva N N, Boris A V, Bernhard C, Kulakov A, Pimenov A, Balbashov A M, Khaliullin G and Keimer B 2004 *Phys. Rev. Lett.* **93** 147204
[20] Blasco J, Ritter C, Garcia J, de Teresa J, Perez-Cacho J and Ibarra M 2000 *Phys. Rev.* B **62** 5609–18
[21] Zhang S F 1996 *J. Appl. Phys.* **79** 4542–4
[22] Senff D, Aliouane N, Argyriou D N, Hiess A, Regnault L P, Link P, Hradil K, Sidis Y and Braden M 2008 *J. Phys.: Condens. Matter* **20** 434212